

W. T. ~~ACR 12~~

T.N. 1699

NATIONAL ADVISORY COMMITTEE FOR AERONAUTICS

TECHNICAL NOTE

No. 1699

A LINEARIZED SOLUTION FOR TIME-DEPENDENT VELOCITY
POTENTIALS NEAR THREE-DIMENSIONAL WINGS AT
SUPERSONIC SPEEDS

By John C. Evvard

Flight Propulsion Research Laboratory
Cleveland, Ohio



Washington
September 1948

Reproduced From
Best Available Copy

20000808 155

AQ M00-11-3668

ERRATA

NACA TN No. 1699

A LINEARIZED SOLUTION FOR TIME-DEPENDENT VELOCITY
POTENTIALS NEAR THREE-DIMENSIONAL WINGS AT
SUPERSONIC SPEEDS

By John C. Ewvard

September 1948

Page 19, equation (31): A plus sign should replace the minus sign of the fourth term within the bracket; that is

$$\phi_T = \frac{2U}{M\alpha} \left\{ \alpha + m t - \frac{m}{4\beta c} (k_1 + 1) u_w + \frac{m}{4\beta c} \left(\frac{1}{k_1} - \frac{2}{3} \right) v_w + \dots \right\}$$

NATIONAL ADVISORY COMMITTEE FOR AERONAUTICS

TECHNICAL NOTE No. 1699

A LINEARIZED SOLUTION FOR TIME-DEPENDENT VELOCITY

POTENTIALS NEAR THREE-DIMENSIONAL WINGS AT

SUPERSONIC SPEEDS

By John C. Evvard

SUMMARY

A source-distribution method is applied to derive a solution for the time-dependent surface velocity potential of thin finite wings at supersonic speeds. The solution is illustrated by evaluating the upwash over the tip of an arbitrary-plan-boundary wing having a supersonic and subsonic leading edge. The upwash then gives the effective sources of the flow field lying between the wing plan boundary and the foremost Mach waves, which are applied in the derivation of the wing-surface velocity potential. A simple example, the load distribution on a wing whose effective angle of attack is changing linearly with time, is included to illustrate the applications of the derived expressions.

INTRODUCTION

The analysis of the aerodynamic effects in the vicinity of thin wings at supersonic speeds can be simplified to obtain useful results by means of the linearized theory. Steady-state or time-independent solutions have been obtained for enough cases (for example, references 1 to 27) that the essential features of the load distributions on various parts of the wing can be determined by graphical or analytical methods. The time-dependent load distributions are more difficult to obtain. Such problems include the transient effects of gusts, changes in angle of attack, skin vibration, and flutter.

A number of investigators have studied two-dimensional time-dependent flows over thin wings. These flows are generally included as special cases of the theory of reference 27. The method of reference 27 is similar to the steady-state solution of reference 1 and includes three-dimensional or finite wing solutions in cases where the aerodynamic effects of the bottom and top wing surfaces are independent. No solutions are known to have been published for cases involving interaction between the flow over the bottom and top wing surfaces.

The concepts of references 9 and 18 that lead to solutions, which include the effects of interaction between the bottom and top wing surfaces in the steady state, can also be applied to obtain time-dependent solutions. The derivation of the surface velocity potential in regions influenced by subsonic leading edges was completed during January 1948 at the NACA Cleveland laboratory and is presented herein.

ANALYSIS

In order to unify the discussion, parts of the fundamental treatment presented in reference 27 are repeated. The analysis includes the derivations of (1) the time-dependent, linearized partial-differential equation for the perturbation-velocity potential of an ideal fluid, (2) the fundamental solution that will satisfy the boundary conditions on the wing, (3) the upwash between the wing boundary and the foremost Mach line, and (4) the velocity potential on the surface of the wing.

Differential equation. - The linearized Euler's equations for a compressible fluid may be written

$$\begin{aligned}\frac{\partial^2 \varphi}{\partial x \partial t} + U \frac{\partial^2 \varphi}{\partial x^2} &= - \frac{1}{\rho_0} \frac{\partial p}{\partial x} \\ \frac{\partial^2 \varphi}{\partial y \partial t} + U \frac{\partial^2 \varphi}{\partial x \partial y} &= - \frac{1}{\rho_0} \frac{\partial p}{\partial y} \\ \frac{\partial^2 \varphi}{\partial z \partial t} + U \frac{\partial^2 \varphi}{\partial x \partial z} &= - \frac{1}{\rho_0} \frac{\partial p}{\partial z}\end{aligned}\tag{1}$$

where

φ perturbation-velocity potential
 t time
 U free-stream velocity
 ρ_0 free-stream density

p static pressure

x, y, z Cartesian coordinates (free stream parallel to x axis)

(A complete list of symbols is included in appendix A.)

When equations(1) are multiplied by dx , dy , and dz respectively, added, and integrated, the result is

$$\frac{\partial \varphi}{\partial t} + U \frac{\partial \varphi}{\partial x} + \frac{p}{\rho_0} = -g(t) \quad (2)$$

where $g(t)$ is an integration constant at any given time.

The linearized continuity equation can be written

$$\frac{\partial \rho}{\partial t} + U \frac{\partial \rho}{\partial x} + \rho_0 \left(\frac{\partial^2 \varphi}{\partial x^2} + \frac{\partial^2 \varphi}{\partial y^2} + \frac{\partial^2 \varphi}{\partial z^2} \right) = 0 \quad (3)$$

or, because the velocity of sound c is

$$c^2 = \frac{dp}{d\rho} \approx c_0^2$$

equation (3) becomes

$$\left(\frac{\partial}{\partial t} + U \frac{\partial}{\partial x} \right) \frac{p}{\rho_0 c_0^2} + \frac{\partial^2 \varphi}{\partial x^2} + \frac{\partial^2 \varphi}{\partial y^2} + \frac{\partial^2 \varphi}{\partial z^2} = 0 \quad (3a)$$

Substitution of p/ρ_0 from equation (2) in equation (3) yields

$$(1 - M^2) \frac{\partial^2 \varphi}{\partial x^2} + \frac{\partial^2 \varphi}{\partial y^2} + \frac{\partial^2 \varphi}{\partial z^2} = \frac{1}{c^2} \frac{\partial^2 \varphi}{\partial t^2} + \frac{2U}{c^2} \frac{\partial^2 \varphi}{\partial x \partial t} + \frac{1}{c^2} \frac{dg}{dt} \quad (4)$$

where M is the Mach number of the free stream and the zero subscript has been dropped from c .

Equation (4) is the required linearized partial-differential equation for the velocity potential. If φ is independent of time, the Prandtl-Glauert equation immediately results.

The function $g(t)$ depends on the condition of the flow ahead of the body. If the flow is uniform and undisturbed, g will be constant (from equation (2)) and equal to p_0/ρ_0 . The function g will be assumed constant in the rest of the analysis.

A change in variables will convert equation (4) to a standard form of the wave equation. The transformation equations are

$$\begin{aligned}x' &= x \\y' &= \sqrt{1 - M^2} y \\z' &= \sqrt{1 - M^2} z \\t' &= (1 - M^2) t + \frac{xM}{c}\end{aligned}\quad (5)$$

Application of equation (5) in equation (4), with g set equal to a constant, gives

$$\frac{\partial^2 \varphi}{\partial x'^2} + \frac{\partial^2 \varphi}{\partial y'^2} + \frac{\partial^2 \varphi}{\partial z'^2} = \frac{1}{c^2} \frac{\partial^2 \varphi}{\partial t'^2} \quad (6)$$

Basic solutions of equation (6) corresponding to spherical waves are

$$\varphi = \frac{1}{r'} f\left(\frac{r'}{\beta^2 c} - \frac{t'}{\beta^2}\right) \quad \text{and} \quad \varphi = \frac{1}{r'} f\left(-\frac{r'}{\beta^2 c} - \frac{t'}{\beta^2}\right) \quad (7)$$

where $r' = \sqrt{x'^2 + y'^2 + z'^2}$, $\beta^2 = M^2 - 1$, and f is an arbitrary function.

The basic solution for the supersonic case is obtained as the sum of equations (7). (See reference 27.) If this solution is transformed to a general point in the x, y, z space, the basic solution of equation (4) assumes the form

$$\varphi = \frac{1}{\sqrt{(x-\xi)^2 - \beta^2(y-\eta)^2 - \beta^2(z-\zeta)^2}} \left[f(\xi, \eta, \zeta, t) - \frac{(x-\xi)M}{\beta^2 c} + \frac{\sqrt{(x-\xi)^2 - \beta^2(y-\eta)^2 - \beta^2(z-\zeta)^2}}{\beta^2 c} \right] + f(\xi, \eta, \zeta, t) - \frac{(x-\xi)M}{\beta^2 c} - \frac{\sqrt{(x-\xi)^2 - \beta^2(y-\eta)^2 - \beta^2(z-\zeta)^2}}{\beta^2 c} \quad (8)$$

where ξ, η , and ζ are Cartesian coordinates in the x, y , and z directions, respectively. Because the operations indicated in equation (4) are independent of ξ, η , and ζ , f may be a function of these variables. Extended solutions of equation (8) may be obtained by integration with respect to any of the variables ξ, η , or ζ .

For thin wings, the sources of the disturbances will lie in the plane of the wing, which may be defined by the relation $\zeta = 0$. The problem is then to determine the function f in terms of known or computed wing or streamline deflections.

Required source strength for thin wings. - In order to shorten the equations, the quantity $\sqrt{(x-\xi)^2 - \beta^2(y-\eta)^2 - \beta^2 z^2}$ may be replaced by the symbol r . Equation (8) then becomes

$$\varphi = \frac{1}{r} \left[f(\xi, \eta, \zeta, t) - \frac{(x-\xi)M}{\beta^2 c} + \frac{r}{\beta^2 c} \right] + f(\xi, \eta, \zeta, t) - \frac{(x-\xi)M}{\beta^2 c} - \frac{r}{\beta^2 c} \quad (8a)$$

The perturbation-velocity component $\partial\varphi/\partial z$ may be obtained by differentiation to give

$$\frac{\partial \varphi}{\partial z} = -\frac{\beta^2 z}{r} \frac{\partial \varphi}{\partial r} \quad (9)$$

The wing dictates that $\partial \varphi / \partial z$ is not zero near $z = 0$. Equation (9), however, shows that the contribution of the sources to $\partial \varphi / \partial z$ is zero, except for those sources near $r = 0$. The quantity r is nearly zero either for small values of $(x-\xi)$, $(y-\eta)$, and z or for $(x-\xi)^2 \approx \beta^2[(y-\eta)^2 + z^2]$. The second condition gives a lower-order zero in the denominator of equation (9) than the first condition and does not contribute to the value of $\partial \varphi / \partial z$ at the point $(x, y, 0)$ on the wing surface.

Near the point $(x, y, 0)$ the quantities $(x-\xi)$ and r are nearly zero. The function f then reduces to a function of x, y , and t . The velocity potential at point (x, y) due to the subelements in the vicinity of the point can then be obtained by integration of the sources included in the forward Mach cone. From figure 1, the field of integration is bounded by the curves $\xi = \xi_1$ and $(x-\xi)^2 - \beta^2(y-\eta)^2 - \beta^2 z^2 = 0$. The velocity potential is then

$$\varphi = 2f(x, y, t) \int_{\xi_1}^{x-\beta z} \int_{\left(y + \frac{1}{\beta} \sqrt{(x-\xi)^2 - \beta^2 z^2}\right)}^{\xi} d\xi \int_{\left(y - \frac{1}{\beta} \sqrt{(x-\xi)^2 - \beta^2 z^2}\right)}^{\eta} \frac{d\eta}{\sqrt{(x-\xi)^2 - \beta^2(y-\eta)^2 - \beta^2 z^2}} \quad (10)$$

$$= \frac{2\pi f(x, y, t)}{\beta} (x - \beta z - \xi_1) \quad (10)$$

Partial differentiation of equation (10) with respect to z gives

$$\frac{\partial \varphi}{\partial z} = w(x, y, t) = -2\pi f(x, y, t) \quad (11)$$

where w is the local z component of the perturbation velocity. Equation (11) defines the strength of the local source in terms of the z component of the perturbation velocity. The fact that equation (11) is independent of the value of ξ_1 is in agreement with the statement that only those subelements near the point $(x, y, 0)$ contribute to the vertical velocity $\partial\phi/\partial z$ on the wing surface. Physically, this evaluation infers that the flow is tangent to the wing surface at each local point.

The time-delay terms of equation (8) can be denoted by τ_a and τ_b where

$$\tau_a = \frac{(x-\xi)M}{\beta^2 c} + \frac{\sqrt{(x-\xi)^2 - \beta^2(y-\eta)^2 - \beta^2 z^2}}{\beta^2 c}$$

$$\tau_b = \frac{(x-\xi)M}{\beta^2 c} - \frac{\sqrt{(x-\xi)^2 - \beta^2(y-\eta)^2 - \beta^2 z^2}}{\beta^2 c} \quad (12)$$

The velocity potential at any point (x, y) is obtained by integrating the sources in the $z = 0$ plane over the area S included in the forward Mach cone. By use of equation (11), the velocity potential becomes

$$\phi = -\frac{1}{2\pi} \iint_S \frac{[w(\xi, \eta, t-\tau_a) + w(\xi, \eta, t-\tau_b)] d\xi d\eta}{\sqrt{(x-\xi)^2 - \beta^2(y-\eta)^2 - \beta^2 z^2}} \quad (13)$$

Equation (13) was derived by Garrick and Rubinow in reference 27 and gives the velocity potential at any point in space in terms of the z component of the perturbation velocity in the $z = 0$ plane. The equation reduces to the steady-state solution of Puckett (reference 1) when w is independent of time.

A physical interpretation may be given for the time delays τ_a and τ_b of equations (12) and (13). If a disturbance is generated at point (ξ, η) at time $t = 0$, the wave front from that disturbance

will travel outward as a spherical wave about a center that moves with the free-stream velocity. (The trace of the waves on the $z = 0$ plane is illustrated in fig. 2.) The wave front will enter and emerge from the point (x, y, z) at two later times τ_a and τ_b . The equation of the spherical wave path that passes through the point (x, y, z) is

$$(x - \xi - U\tau)^2 + (y - \eta)^2 + z^2 = c^2\tau^2 \quad (14)$$

The solution for τ is

$$\tau = \frac{(x - \xi)M}{\beta^2 c} \pm \frac{\sqrt{(x - \xi)^2 - \beta^2(y - \eta)^2 - \beta^2 z^2}}{\beta^2 c}$$

which gives equations (12). (At a given point (x, y, z) , the strengths of the same wave at the two times τ_a and τ_b are equal despite the change in the radius of the wave front.) At a given time t , only the wave fronts that are entering and emerging from the point (x, y, z) contribute to the velocity potential. These two waves originated at the point $(\xi, \eta, 0)$ at times $(t - \tau_a)$ and $(t - \tau_b)$.

The remainder of the analysis is primarily concerned with the aerodynamics in the plane of the wing so that z may be set equal to zero. Equations (12) and (13) may also be conveniently expressed in an oblique coordinate system whose axes lie parallel to the Mach lines. (See fig. 3.) The transformation equations are

$$\begin{aligned} u &= \frac{M}{2\beta} (\xi - \beta\eta) & v &= \frac{M}{2\beta} (\xi + \beta\eta) \\ \xi &= \frac{\beta}{M} (v + u) & \eta &= \frac{1}{M} (v - u) \\ u_w &= \frac{M}{2\beta} (x - \beta y) & v_w &= \frac{M}{2\beta} (x + \beta y) \\ x &= \frac{\beta}{M} (v_w + u_w) & y &= \frac{1}{M} (v_w - u_w) \end{aligned} \quad (15)$$

Inasmuch as the elemental area in the (u, v) coordinate system is

$\frac{2\beta}{M^2} du dv$, equations (13) and (12), in the case of $z = 0$, become

$$\varphi = - \frac{1}{2M\pi} \iint_S \frac{[w(u,v,t-\tau_a) + w(u,v,t-\tau_b)] du dv}{\sqrt{(u_w-u)(v_w-v)}} \quad (16)$$

$$\tau_a = \frac{M(v_w-v+u_w-u) + 2\sqrt{(u_w-u)(v_w-v)}}{M\beta c}$$

$$\tau_b = \frac{M(v_w-v+u_w-u) - 2\sqrt{(u_w-u)(v_w-v)}}{M\beta c} \quad (17)$$

Equation (16) gives the velocity potential in the $z = 0$ plane in terms of the perturbation-velocity component w normal to the plane. If only supersonic leading edges are included in the forward Mach cone from (x,y) , w may be evaluated in terms of the effective wing slopes σ measured in $\eta = \text{constant}$ planes by the relation

$$w = U\sigma \quad (18)$$

If a subsonic leading (or trailing) edge is also included in the forward Mach cone from (x,y) , the slopes of the stream-lines λ associated with the upwash between the wing boundary and the foremost Mach wave must be evaluated and included in the calculation (equation (16)) for the velocity potential.

Upwash between wing boundary and foremost Mach line. - The slopes of the streamlines in the region S_D of figure 4 could conceivably be generated by a thin wing or diaphragm, as employed in reference 9. The flows above and below the $z = 0$ plane may then be independently treated. The velocity potential on the top surface of the $z = 0$ plane is given by equations (16) and (18) as

$$\begin{aligned}
\varphi_T = & -\frac{U}{2M\pi} \iint_{S_w} \frac{[\sigma_T(u,v,t-\tau_a) + \sigma_T(u,v,t-\tau_b)]}{\sqrt{(u_D-u)(v_D-v)}} du dv \\
& -\frac{U}{2M\pi} \iint_{S_D} \frac{[\lambda(u,v,t-\tau_a) + \lambda(u,v,t-\tau_b)]}{\sqrt{(u_D-u)(v_D-v)}} du dv \quad (19)
\end{aligned}$$

where u_D and v_D are the coordinates of the point at which φ is evaluated, σ_T represents the slopes of the streamlines on the top wing surface, and λ represents the slopes of the streamlines in the field S_D from the point of view of the top wing surface. Similarly, the potential on the bottom surface of the $z = 0$ plane is

$$\begin{aligned}
\varphi_B = & -\frac{U}{2M\pi} \iint_{S_w} \frac{[\sigma_B(u,v,t-\tau_a) + \sigma_B(u,v,t-\tau_b)]}{\sqrt{(u_D-u)(v_D-v)}} du dv \\
& -\frac{U}{2M\pi} \iint_{S_D} \frac{-[\lambda(u,v,t-\tau_a) + \lambda(u,v,t-\tau_b)]}{\sqrt{(u_D-u)(v_D-v)}} du dv \quad (20)
\end{aligned}$$

The pressure at a given point of the field S_D (fig. 4) in the plane of the wing can be calculated by substituting either φ_T or φ_B into equation (2). The two computations of the pressure can then be equated:

$$\frac{\partial \varphi_T}{\partial t} + U \frac{\partial \varphi_T}{\partial x} = \frac{\partial \varphi_B}{\partial t} + U \frac{\partial \varphi_B}{\partial x} \quad (21)$$

Equation (21) has the solution

$$\varphi_T = \varphi_B + 2H(x-Ut, y) \quad (21a)$$

where H is an integration function. Substitution of equations (19) and (20) in (21a) yields

$$-\frac{U}{2M\pi} \iint_{S_D} \frac{\lambda_{a,b} \, du \, dv}{\sqrt{(u_D-u)(v_D-v)}} = -\frac{U}{2M\pi} \iint_{S_w} \frac{(\sigma_B - \sigma_T)_{a,b} \, du \, dv}{2 \sqrt{(u_D-u)(v_D-v)}} + H \quad (21b)$$

(In equation (21b) and in some of the equations to follow, the notation λ_a means $\lambda(u, v, t - \tau_a)$ and $\lambda_{a,b}$ means $[\lambda(u, v, t - \tau_a) + \lambda(u, v, t - \tau_b)]$. A similar notation is applied to σ_B , σ_T , and $(\sigma_B - \sigma_T)$.) If equation (21b) is substituted into (19), the result is

$$\varphi_T = -\frac{U}{2M\pi} \iint_{S_w} \frac{(\sigma_B + \sigma_T)_{a,b} \, du \, dv}{2 \sqrt{(u_D-u)(v_D-v)}} + H \quad (22)$$

Equation (22) represents the velocity potential in the plane of the wing for the region S_D . Similarly, formulation of φ_B would change only the sign affixed to H . The function $2H$ of equation (21a) represents the difference in potential across the $z = 0$ plane, corresponding to the strength of vorticity in the wake of the wing (reference 18). For flat-plate wings, $\sigma_B + \sigma_T = 0$ and H is just the potential on the top surface of the vortex sheet.

The foremost Mach wave (fig. 4 or 5) originating on the leading edge generally represents a line of infinitesimal disturbance along which $H(x-Ut, y)$ can be set equal to zero at all times. The function H remains zero along $y = \text{constant}$ lines for values of x not intercepted by the wing or a material body (region $S_{D,1}$ of fig. 5). The region $S_{D,2}$ of figure 5 generally contains a vortex

sheet lying in the plane of the wing and H is not zero. The function $H(y)$, established along the wing trailing edge at some time t , remains unaltered for later times along a curve that sweeps downstream with the free-stream velocity and has the form of the wing trailing edge. The rest of the discussion is concerned with only the effects of leading edges, that is, those cases for which H is zero.

The origin of coordinates for the wing shown on figure 4 is placed at the junction of the supersonic and subsonic leading edge. The supersonic and subsonic leading edges are respectively defined by the equations

$$\begin{aligned} v &= v_1(u) & \text{or} & & u &= u_1(v) \\ v &= v_2(u) & \text{or} & & u &= u_2(v) \end{aligned} \quad (23)$$

Equation (21b) with H set equal to zero, then becomes

$$\int_0^{u_D} \frac{du}{\sqrt{u_D-u}} \int_{v_2(u)}^{v_D} \frac{\lambda_{a,b} dv}{\sqrt{v_D-v}} = \int_0^{u_D} \frac{du}{\sqrt{u_D-u}} \int_{v_1(u)}^{v_2(u)} \frac{(\sigma_B - \sigma_T)_{a,b} dv}{2\sqrt{v_D-v}} \quad (21c)$$

In the steady-state solution, λ and $(\sigma_B - \sigma_T)$ are independent of u_D (references 9 and 11), so that the integrations with respect to v may be equated to give

$$\int_{v_2(u)}^{v_D} \frac{\lambda_{a,b} dv}{\sqrt{v_D-v}} = \int_{v_1(u)}^{v_2(u)} \frac{(\sigma_B - \sigma_T)_{a,b} dv}{2\sqrt{v_D-v}} \quad (24)$$

The reduction of equation (21c) to give equation (24) for the time-independent case shows that only those wing slopes along $u = u_D$ contribute to the upwash for points on this Mach line. In the time-dependent case, both λ and $(\sigma_B - \sigma_T)$ contain functions of u_D , and the validity of the reduction may be questioned. If

in the time-dependent case only those wing slopes along $u = u_D$ were to contribute to the upwash for points on this Mach line, λ and $(\sigma_B - \sigma_T)$ would become independent of u_D and the reduction of equation (21c) to equation (24) would again be justified. An argument to substantiate this choice is presented in appendix B.

If u is replaced by u_D in equation (24), the two time delays become equal and are linear with respect to v :

$$\tau_a = \tau_b = \frac{v_D - v}{\beta c}$$

Each infinitesimal wing element then produces at time t and place v_D an increment in upwash corresponding to the steady-state effect of wing elements whose slopes are the same as the time-dependent elements evaluated at time $t - \tau_a$. The solution of equation (24) is the sum of a series of infinitesimal steady-state solutions, each of which satisfies Abel's equation (reference 11) and each of which requires integration only over the wing slopes along $u = u_D$.

In order to illustrate the argument, the increment in λ at point (u_D, v_D) (fig. 6) due to a steady-state wing element of length dv at point (u_D, v) may be obtained (appendix B) from Abel's equation in the manner of reference 11 as

$$\frac{d\lambda}{dv} = \frac{(\sigma_B - \sigma_T) \sqrt{v_D - v}}{2\pi(v_D - v) \sqrt{v_D - v_2}} \quad (25)$$

Equation (25) may be applied in either the time-dependent or the time-independent cases. For the time-independent cases, the wing slopes are evaluated at u_D, v . For the time-dependent solutions, the wing slopes are evaluated at (u_D, v) at time $t - \frac{v_D - v}{\beta c}$.

Integration of equation (25) across the wing gives

$$\lambda(u, v_D, t) = \frac{1}{2\pi \sqrt{v_D - v_2}} \int_{v_1}^{v_2} \frac{\sigma_{B,T} \left(u, v, t - \frac{v_D - v}{\beta c} \right) \sqrt{v_2 - v} dv}{v_D - v} \quad (26)$$

974

where $\sigma_{B,T}$ means $(\sigma_B - \sigma_T)$. That equation (26) is a solution of equation (24) is shown in appendix B.

Evaluation of velocity potential on wing surface. - Equations (19) and (26) now allow the calculations of the velocity potential on the wing surface. With reference to figure 7, the velocity potential at the point (u_w, v_w) is

$$\varphi_T = - \frac{U}{2M\pi} \iint_{S_{w,1+2}} \frac{\sigma_{T,a,b} du dv}{\sqrt{(u_w - u)(v_w - v)}} - \frac{U}{2M\pi} \iint_{S_D} \frac{\lambda_{a,b} du dv}{\sqrt{(u_w - u)(v_w - v)}} \quad (27)$$

For the wing of figure 7, the integration of λ over the area S_D is

$$\begin{aligned} I &= - \frac{U}{2M\pi} \iint_{S_D} \frac{\lambda_{a,b} du dv}{\sqrt{(u_w - u)(v_w - v)}} \\ &= - \frac{U}{2M\pi} \int_0^{u_2(v_w)} \frac{du}{\sqrt{(u_w - u)}} \int_{v_2}^{v_w} \frac{\lambda_{a,b} dv_D}{\sqrt{v_w - v_D}} \end{aligned} \quad (28)$$

If λ from equation (26) is substituted into equation (28), there results

$$I = -\frac{U}{4\pi^2 M} \int_0^{u_2(v_w)} \frac{du}{\sqrt{u_w - u}} \int_{v_1(u)}^{v_w} \frac{dv}{\sqrt{(v_D - v_2)(v_w - v_D)}} \int_{v_1(u)}^{v_2(u)} \frac{dv}{\sqrt{(v_D - v_2)(v_w - v_D)}} \frac{\sqrt{v_2 - v} \sigma_{B,T} \left[u, v, t - \frac{v_w - v}{\beta c} - \frac{u_w - u}{\beta c} - \frac{2}{\beta M c} \sqrt{(u_w - u)(v_w - v_D)} \right] dv}{v_D - v}$$

$$- \frac{U}{4\pi^2 M} \int_0^{u_2(v_w)} \frac{du}{\sqrt{u_w - u}} \int_{v_1(u)}^{v_w} \frac{dv}{\sqrt{(v_D - v_2)(v_w - v_D)}} \int_{v_1(u)}^{v_2(u)} \frac{dv}{\sqrt{(v_D - v_2)(v_w - v_D)}} \frac{\sqrt{v_2 - v} \sigma_{B,T} \left[u, v, t - \frac{v_w - v}{\beta c} - \frac{u_w - u}{\beta c} + \frac{2}{\beta M c} \sqrt{(u_w - u)(v_w - v_D)} \right] dv}{v_D - v}$$

(28a)

The integration of λ over the flow field S_D can be replaced by the integration of a function over the wing area $S_{w,1}$. This replacement is accomplished by interchanging the order of integration of v and v_D . Equation (28a) then becomes

$$I = -\frac{U}{4\pi^2 M} \int_0^{u_2(v_w)} \frac{du}{\sqrt{u_w - u}} \int_{v_1(u)}^{v_2(u)} \frac{dv}{\sqrt{v_2 - v}} \int_{v_1(u)}^{v_w} \frac{dv}{\sqrt{(v_D - v_2)(v_w - v_D)}} \frac{\sqrt{v_2 - v} \sigma_{B,T} \left[u, v, t - \frac{v_w - v}{\beta c} - \frac{u_w - u}{\beta c} - \frac{2}{\beta M c} \sqrt{(u_w - u)(v_w - v_D)} \right] dv_D}{(v_D - v) \sqrt{(v_D - v_2)(v_w - v_D)}}$$

$$- \frac{U}{4\pi^2 M} \int_0^{u_2(v_w)} \frac{du}{\sqrt{u_w - u}} \int_{v_1(u)}^{v_2(u)} \frac{dv}{\sqrt{v_2 - v}} \int_{v_1(u)}^{v_w} \frac{dv}{\sqrt{(v_D - v_2)(v_w - v_D)}} \frac{\sqrt{v_2 - v} \sigma_{B,T} \left[u, v, t - \frac{v_w - v}{\beta c} - \frac{u_w - u}{\beta c} + \frac{2}{\beta M c} \sqrt{(u_w - u)(v_w - v_D)} \right] dv_D}{(v_D - v) \sqrt{(v_D - v_2)(v_w - v_D)}}$$

(28b)

Equation (28b) represents the contribution to the velocity potential of the upwash over the wing tip and can be used to rewrite parts of equation (27). If the velocity potential from equation (27) is written in full for the wing of figure 7, the following results are obtained:

$$\begin{aligned} \varphi_T = & -\frac{U}{2M\alpha} \int_0^{u_2(v_w)} \frac{du}{\sqrt{u_w-u}} \int_{v_1(u)}^{v_2(u)} \sigma_T \left[u, v, t, -\frac{v_w-v}{\beta c} - \frac{u_w-u}{\beta c} - \frac{2}{\beta M c} \sqrt{(u_w-u)(v_w-v)} \right] dv \\ & -\frac{U}{2M\alpha} \int_0^{u_2(v_w)} \frac{du}{\sqrt{u_w-u}} \int_{v_1(u)}^{v_2(u)} \sigma_T \left[u, v, t, -\frac{v_w-v}{\beta c} - \frac{u_w-u}{\beta c} + \frac{2}{\beta M c} \sqrt{(u_w-u)(v_w-v)} \right] dv \\ & -\frac{U}{2M\alpha} \int_{u_2(v_w)}^{u_w} \frac{du}{\sqrt{u_w-u}} \int_{v_1(u)}^{v_w} \sigma_T \left[u, v, t, -\frac{v_w-v}{\beta c} - \frac{u_w-u}{\beta c} - \frac{2}{\beta M c} \sqrt{(u_w-u)(v_w-v)} \right] dv \\ & -\frac{U}{2M\alpha} \int_{u_2(v_w)}^{u_w} \frac{du}{\sqrt{u_w-u}} \int_{v_1(u)}^{v_w} \sigma_T \left[u, v, t, -\frac{v_w-v}{\beta c} - \frac{u_w-u}{\beta c} + \frac{2}{\beta M c} \sqrt{(u_w-u)(v_w-v)} \right] dv \end{aligned}$$

(continued on the following page)

$$\begin{aligned}
 & - \frac{U}{4\pi^2 M} \int_0^{u_2(v_w)} \frac{du}{\sqrt{u_w - u}} \int_{v_1(u)}^{v_2(u)} \sqrt{v_2 - v} \, dv \int_{v_w}^v \sigma_B \left[u, v, t, -\frac{v_w - v}{\beta c} - \frac{u_w - u}{\beta c} - \frac{2}{\beta M c} \sqrt{(u_w - u)(v_w - v_D)} \right] dv_D \\
 & \quad \quad \quad (v_D - v) \sqrt{(v_D - v_2)(v_w - v_D)} \\
 & + \frac{U}{4\pi^2 M} \int_0^{u_2(v_w)} \frac{du}{\sqrt{u_w - u}} \int_{v_1(u)}^{v_2(u)} \sqrt{v_2 - v} \, dv \int_{v_w}^v \sigma_T \left[u, v, t, -\frac{v_w - v}{\beta c} - \frac{u_w - u}{\beta c} - \frac{2}{\beta M c} \sqrt{(u_w - u)(v_w - v_D)} \right] dv_D \\
 & \quad \quad \quad (v_D - v) \sqrt{(v_D - v_2)(v_w - v_D)} \\
 & - \frac{U}{4\pi^2 M} \int_0^{u_2(v_w)} \frac{du}{\sqrt{u_w - u}} \int_{v_1(u)}^{v_2(u)} \sqrt{v_2 - v} \, dv \int_{v_w}^v \sigma_B \left[u, v, t, -\frac{v_w - v}{\beta c} - \frac{u_w - u}{\beta c} + \frac{2}{\beta M c} \sqrt{(u_w - u)(v_w - v_D)} \right] dv_D \\
 & \quad \quad \quad (v_D - v) \sqrt{(v_D - v_2)(v_w - v_D)} \\
 & + \frac{U}{4\pi^2 M} \int_0^{u_2(v_w)} \frac{du}{\sqrt{u_w - u}} \int_{v_1(u)}^{v_2(u)} \sqrt{v_2 - v} \, dv \int_{v_w}^v \sigma_T \left[u, v, t, -\frac{v_w - v}{\beta c} - \frac{u_w - u}{\beta c} + \frac{2}{\beta M c} \sqrt{(u_w - u)(v_w - v_D)} \right] dv_D \\
 & \quad \quad \quad (v_D - v) \sqrt{(v_D - v_2)(v_w - v_D)}
 \end{aligned}$$

(27a)

Although equation (27a) looks rather formidable, there are actually only two types of term. Simple variations are obtained by changing signs from minus to plus, by replacing bottom-surface wing slopes by top-surface wing slopes, or by altering the limits of integration. Simplifications also occur in specific examples, although the indicated integrations to obtain explicit solutions are generally difficult to perform.

If the wing slopes in the vicinity of the wing tip vary continuously with either time or position, equation (27a) can be applied in its present form without altering the limits of integration. The equations for the wing slope would be inserted into equation (27a) and the indicated integrations conducted. This type of calculation has been illustrated for periodic oscillations of flat-plate wings in references 27 and 28 when the bottom- and top-wing slopes are independent. A less complicated example, in which the angle of attack of all wing elements of a flat plate varies linearly with time, illustrates this type of calculation.

If the angle of attack of all wing elements is changed at a uniform rate m for all times, the wing slopes may be expressed as

$$\sigma_B = \alpha + mt = -\sigma_T \quad (29)$$

where α is the angle of attack of the wing at time $t = 0$. These effective wing slopes may correspond to a constant acceleration of mU in the z direction. Substitution of equation (29) into equation (27a) gives

$$\begin{aligned} \varphi_T = & \frac{U\alpha}{M\pi} \int_{u_2(v_w)}^{u_w} \frac{du}{\sqrt{u_w - u}} \int_{v_1(u)}^{v_w} \frac{dv}{\sqrt{v_w - v}} \\ & + \frac{Um}{M\pi} \int_{u_2(v_w)}^{u_w} \frac{du}{\sqrt{u_w - u}} \int_{v_1(u)}^{v_w} \frac{\left(t - \frac{v_w - v}{\beta c} - \frac{u_w - u}{\beta c}\right) dv}{\sqrt{v_w - v}} \end{aligned} \quad (30)$$

Integration with respect to v produces

$$\begin{aligned} \varphi_T = \frac{2U}{M\pi} & \left[(\alpha + mt) \int_{u_2}^{u_w} \frac{\sqrt{v_w - v_1(u)}}{\sqrt{u_w - u}} du - \frac{m}{3\beta c} \int_{u_2}^{u_w} \frac{(v_w - v_1(u))^{\frac{3}{2}}}{\sqrt{u_w - u}} du \right. \\ & \left. - \frac{m}{\beta c} \int_{u_2}^{u_w} \sqrt{(u_w - u)(v_w - v_1(u))} du \right] \end{aligned} \quad (30a)$$

If the equation for the leading edge of the wing is $v = -k_1 u$, equation (30a) may be integrated to obtain

$$\begin{aligned} \varphi_T = \frac{2U}{M\pi} & \left\{ \left[\alpha + mt - \frac{m}{4\beta c} (k_1 + 1)u_w + \frac{m}{4\beta c} \left(\frac{1}{k_1} - \frac{5}{3} \right) v_w \right. \right. \\ & \left. + \frac{m}{2\beta c} \left(1 - \frac{k_1}{3} \right) u_2 \right] \sqrt{(u_w - u_2)(v_w + k_1 u_2)} \\ & \left. + \frac{1}{\sqrt{k_1}} \left[(\alpha + mt)(k_1 u_w + v_w) - \frac{(k_1 + 1)m(k_1 u_w + v_w)^2}{4\beta c k_1} \right] \tan^{-1} \sqrt{\frac{k_1(u_w - u_2)}{v_w + k_1 u_2}} \right\} \end{aligned} \quad (31)$$

The pressure coefficient may be derived from equation (2) as

$$C_p = \frac{p - p_0}{\frac{1}{2}\rho_0 U^2} = -\frac{2}{U} \left(\frac{\partial \varphi}{\partial x} + \frac{1}{U} \frac{\partial \varphi}{\partial t} \right) \quad (32)$$

Substitution of equation (31) into equation (32) results in the pressure coefficient on a family of wings in the region influenced by the subsonic leading edge.

Page 20: Equation (33) should read as follows:

$$\begin{aligned}
 C_p = & -\frac{2}{\beta\pi} \left\{ m \left[\frac{2\beta}{UM} + \frac{(1 - k_1^2)}{2\beta c k_1} \right] \sqrt{(u_w - u_2)(v_w + k_1 u_2)} \right. \\
 & + \frac{1}{\sqrt{k_1}} \left[(k_1 + 1)(\alpha + mt) + m(k_1 u_w + v_w) \left(\frac{2\beta}{UM} - \frac{(k_1 + 1)^2}{2\beta c k_1} \right) \right] \tan^{-1} \sqrt{\frac{k_1(u_w - u_2)}{(v_w + k_1 u_2)}} \\
 & \left. + \left[(\alpha + mt) - \frac{m}{\beta c}(u_w - u_2) - \frac{m}{3\beta c}(v_w + k_1 u_2) \right] \left(1 - \frac{du_2}{dv_w} \right) \sqrt{\frac{v_w + k_1 u_2}{u_w - u_2}} \right\}
 \end{aligned}
 \tag{33}$$

where $u_2(v)$ is evaluated at $v = v_w$. (Although equation (33) was derived for the case of constant acceleration mU in the z direction, the solution may be combined with other equations to evaluate the pressure distributions for a variety of wing motions. For example, a wing rotating with constant rate m about an axis of pitch fixed with respect to the wing and lying in the $z = 0$ plane would have the pressure distribution given by equation (33) superposed on the pressure distribution associated with uniform rates of pitch described in reference 21.)

The steady-state solution included in reference 18 is obtained from equation (33) by setting $m = 0$. The solution for the infinite swept wing is obtained by setting $v_w = u_2(v_w) = 0$ and computing C_p . The values of C_p obtained along the line $v_w = 0$ are then constant along lines parallel to the leading edge. The load distributions of a family of wing plan boundaries may be evaluated by choosing the desired equation $u = u_2(v)$ for the wing-tip plan boundary.

The general equation (27a) also includes solutions for which a finite number of discontinuities can exist in the wing slopes with respect to either position or time. The procedure is the same as in the case of continuous wing slopes, except that the fields

of integration will be subdivided in accordance with the requirement of the discontinuity. For example, in the problem of determining gust loads, the effective angle of attack of the wing will change discontinuously along a line parallel to the y axis that moves downstream with the free-stream velocity. If the initial wing slope is taken as zero and the increment in wing slope due to the gust is α , the slopes of the wing at time $t - \tau$ (as time appears in equation (27a)) are either zero or α according to the inequalities

$$\begin{aligned} \xi > U(t - \tau), & \quad \sigma_B = -\sigma_T = 0 \\ \xi < U(t - \tau), & \quad \sigma_B = -\sigma_T = \alpha \end{aligned}$$

The two-dimensional solution of this problem is presented in reference 29. The three-dimensional solution of this and other transient problems within the scope of equation (27a) requires further research.

Flight Propulsion Research Laboratory,
National Advisory Committee for Aeronautics,
Cleveland, Ohio, May 18, 1948.

APPENDIX A

SYMBOLS

The following symbols are used in this report.

C_p	pressure coefficient, $\frac{p - p_0}{\frac{1}{2} \rho U^2}$
c	velocity of sound
f	function
g	integration function of time (herein considered as constant)
H	integration function of $x-Ut$ and y
I	integral
k_1	constant greater than zero
M	free-stream Mach number
m	rate of increase of wing angle of attack
p	static pressure
$r =$	$\sqrt{(x - \xi)^2 - \beta^2(y - \eta)^2 - \beta^2 z^2}$
$r' =$	$\sqrt{x'^2 + y'^2 + z'^2}$
S	plan-form area
s	manipulation variable
t	time
$t' =$	$(1 - M^2) t + \frac{xM}{c}$
U	free-stream velocity, taken parallel to x axis
u, v	oblique coordinates whose axes lie parallel to Mach lines in $z = 0$ plane

w	z component of perturbation velocity, $\frac{\partial \phi}{\partial z}$ (taken as positive in direction of an outwardly drawn normal from plane of wing)
x,y,z	Cartesian coordinates
x',y',z'	transformed Cartesian coordinates ($x' = x$, $y' = \sqrt{1-M^2}y$, $z' = \sqrt{1-M^2}z$)
ξ, η, ζ	Cartesian coordinates in x,y,z directions, respectively
α	angle of attack
β	cotangent of Mach angle, $\sqrt{M^2 - 1}$
λ	effective slopes of streamlines (measured in $\eta = \text{constant}$ planes) in $z = 0$ plane between wing boundary and foremost Mach line, $\lambda = \frac{w}{U}$
ρ	density
σ	effective wing-section slopes measured in $\eta = \text{constant}$ planes ($\sigma = w/U$)
τ	time delay
ϕ	perturbation-velocity potential
Subscripts:	
0	free stream
1,2,3 . . .	numbered areas or wing-plan-boundary equations
a,b	time delays τ_a and τ_b
B	bottom (of wing)
D	upwash field
T	top (of wing)
w	wing

Examples:

v_1 curve $v = v_1(u)$ along supersonic leading edge

u_2 curve $u = u_2(v)$ along subsonic leading edge

$S_w(1 + 2)$ wing areas 1 plus 2

$\frac{du_2}{dv_w}$ derivative of curve $u_2(v_w)$ with respect to v_w

$\lambda_{a,b}$ slope at time $t - \tau_a$ plus slope at time $t - \tau_b$

$(\sigma_B - \sigma_T)_{a,b}$ difference between bottom and top wing slopes at time $t - \tau_a$ plus this difference at time $t - \tau_b$

$\sigma_{B,T}$ $\sigma_B - \sigma_T$

u_w, v_w oblique coordinates of point x, y on wing

APPENDIX B

EVALUATION OF UPWASH

Origin of upwash. - The fundamental source solution (equation (8)) for the three-dimensional velocity potential of thin wings moving at supersonic speeds can be written as

$$\varphi = \frac{f_{a,b}}{r} \quad (B1)$$

If this equation is partially differentiated with respect to z , the result is

$$\frac{\partial \varphi}{\partial z} = \frac{\partial \varphi}{\partial r} \frac{\partial r}{\partial z} = -\frac{\beta^2 z}{r} \frac{\partial \varphi}{\partial r} \quad (B2)$$

If z is allowed to approach zero, the quantity $\partial \varphi / \partial z$ will approach zero unless $\frac{1}{r} \frac{\partial \varphi}{\partial r}$ approaches infinity (that is, r

approaches zero). The fundamental solution (B1) can then be integrated over a surface of sources in the $z = 0$ plane to obtain an extended velocity potential. Because of the form of equation (B2), the z component of the perturbation velocity generated by this potential will arise only from those subelements near $r = 0$.

On the wing, the flow must be tangent at each point to a defined surface. The quantity $\partial \varphi / \partial z$ is therefore determined at each local point by the wing. Under such circumstances and because of the wing restraint, only the subelements near $r = 0$ obtained by assuming $(x - \xi) \approx (y - \eta) \approx (z - \zeta) \approx 0$ contribute to $\partial \varphi / \partial z$. No such restraint exists for the upwash field. If the same condition is imposed to evaluate $\partial \varphi / \partial z$ in the upwash field part of the $z = 0$ plane, the trivial answer $\frac{\partial \varphi}{\partial z} = \frac{\partial \varphi}{\partial z}$ results.

A fundamental distinction exists between the evaluation of $\partial \varphi / \partial z$ on the surface of the wing and in the upwash field. The wing surface is a restraint and can generate primary impulses that lead to the velocity potential and hence to the flow distributions. The upwash field is unrestrained, however, and can transfer from the bottom to the top wing surfaces only those impulses that have already been generated by the wing.

The upwash must arise, however, from those subelements near $r = 0$. Because the unrestrained subelements in the vicinity of the point $(x - \xi) = (y - \eta) = z = 0$ cannot generate upwash, $\partial\phi/\partial z$ (for $z = 0$) must be generated by those subelements in the vicinity of the curve $(x - \xi)^2 - \beta^2(y - \eta)^2 = \beta^2 z^2 = 0$. This condition implies that only those wing slopes along $u = u_D$ generate the upwash for points on this Mach line. The defining equation for λ should then be restricted by setting $u = u_D$, for either time-independent or time-dependent flows. This result was proved directly from the integral equation (21c) for time-independent cases (reference 11).

Differential equation for λ . - The increment $d\lambda$ at point u_D, v_D due to the wing elements dv (fig. 6) of wing slopes $\frac{\sigma_B - \sigma_T}{2}$ may be determined from equation (6) of reference 11 as

$$d\lambda = \frac{1}{\pi} \frac{\partial}{\partial s} \int_{v_2}^s \frac{dv_D}{\sqrt{s - v_D}} \int_v^{v+dv} \frac{(\sigma_B - \sigma_T)dv}{2\sqrt{v_D - v}} \quad (B3)$$

where s is the manipulation variable and is evaluated at $s = v_D$. The integration of dv over an infinitesimal distance results in the removal of one integration sign. Also, $(\sigma_B - \sigma_T)$ may be considered as constant. Equation (B3) then becomes

$$\begin{aligned} \frac{d\lambda}{dv} &= \frac{\sigma_B - \sigma_T}{2\pi} \frac{\partial}{\partial s} \int_{v_2}^s \frac{dv_D}{\sqrt{(s - v_D)(v_D - v)}} \\ &= \frac{(\sigma_B - \sigma_T)}{2\pi} \frac{\sqrt{v_2 - v}}{(s - v)\sqrt{s - v_2}} \end{aligned} \quad (B3a)$$

Replacement of the manipulation variable s by v_D gives equation (25)

$$\frac{d\lambda}{dv} = \frac{(\sigma_B - \sigma_T)}{2\pi} \frac{\sqrt{v_2 - v}}{(v_D - v)\sqrt{v_D - v_2}} \quad (B3b)$$

Demonstration by substitution that equation (26) satisfies equation (24) when $u = u_D$. - If the integration variable v is changed to s to prevent confusion, equation (26) assumes the following form:

$$\lambda(u, v, t) = \frac{1}{2\pi\sqrt{v-v_2}} \int_{v_1}^{v_2} \frac{\sigma_{B,T}\left(u, s, t - \frac{v-s}{\beta c}\right) \sqrt{v_2-s} \, ds}{v-s} \quad (B4)$$

Therefore

$$\lambda\left(u, v, t - \frac{v_D-v}{\beta c}\right) = \frac{1}{2\pi\sqrt{v-v_2}} \int_{v_1}^{v_2} \frac{\sigma_{B,T}\left(u, s, t - \frac{v_D-s}{\beta c}\right) \sqrt{v_2-s} \, ds}{v-s} \quad (B5)$$

The first member of equation (24) then becomes

$$\begin{aligned} \int_{v_2}^{v_D} \frac{\lambda_{a,b} dv}{\sqrt{v_D-v}} &= \frac{1}{\pi} \int_{v_2}^{v_D} \frac{dv}{\sqrt{(v-v_2)(v_D-v)}} \int_{v_1}^{v_2} \frac{\sigma_{B,T}\left(u, s, t - \frac{v_D-s}{\beta c}\right) \sqrt{v_2-s} \, ds}{v-s} \\ &= \frac{1}{\pi} \int_{v_1}^{v_2} \sigma_{B,T}\left(u, s, t - \frac{v_D-s}{\beta c}\right) \sqrt{v_2-s} \, ds \int_{v_2}^{v_D} \frac{dv}{(v-s) \sqrt{(v-v_2)(v_D-v)}} \end{aligned} \quad (B6)$$

According to integral 195 of reference 30, however,

$$\int_{v_2}^{v_D} \frac{dv}{(v-s) \sqrt{(v-v_2)(v_D-v)}} = \frac{\pi}{\sqrt{(v_2-s)(v_D-s)}}$$

Therefore

$$\begin{aligned} \int_{v_2}^{v_D} \frac{\lambda_{a,b} dv}{\sqrt{v_D - v}} &= \int_{v_1}^{v_2} \frac{\sigma_{B,T} \left(u, s, t - \frac{v_D - s}{\beta c} \right) ds}{\sqrt{v_D - s}} \\ &= \int_{v_1}^{v_2} \frac{(\sigma_B - \sigma_T)_{a,b} dv}{2 \sqrt{v_D - v}} \end{aligned} \quad (B7)$$

Equation (B7) is equation (24) for $u = u_D$.

REFERENCES

1. Puckett, Allen E.: Supersonic Wave Drag of Thin Airfoils. Jour. Aero. Sci., vol. 13, no. 9, Sept. 1946, pp. 475-484.
2. Jones, Robert T.: Thin Oblique Airfoils at Supersonic Speed. NACA TN No. 1107, 1946.
3. Stewart, H. J.: The Lift of a Delta Wing at Supersonic Speeds. Quarterly Appl. Math., vol. IV, no. 3, Oct. 1946, pp. 246-254.
4. Brown, Clinton E.: Theoretical Lift and Drag of Thin Triangular Wings at Supersonic Speeds. NACA TN No. 1183, 1946.
5. Ackeret, J.: Air Forces on Airfoils Moving Faster Than Sound. NACA TM No. 317, 1925.
6. Busemann, Adolf: Infinitesimal Conical Supersonic Flow. NACA TM No. 1100, 1947.
7. Bonney, E. Arthur: Aerodynamic Characteristics of Rectangular Wings at Supersonic Speeds. Jour. Aero. Sci., vol. 14, no. 2, Feb. 1947, pp. 110-116.
8. Lighthill, M. J.: The Supersonic Theory of Wings of Finite Span. R. & M. No. 2001, A.R.C., 1944.
9. Evvard, John C.: Distribution of Wave Drag and Lift in the Vicinity of Wing Tips at Supersonic Speeds. NACA TN No. 1382, 1947.
10. Evvard, John C.: The Effects of Yawing Thin Pointed Wings at Supersonic Speeds. NACA TN No. 1429, 1947.
11. Evvard, John C. and Turner, L. Richard: Theoretical Lift Distribution and Upwash Velocities for Thin Wings at Supersonic Speeds. NACA TN No. 1484, 1947.
12. Moeckel, W. E.: Effect of Yaw at Supersonic Speeds on the Theoretical Aerodynamic Coefficients of Thin Pointed Wings with Several Types of Trailing Edge. NACA TN No. 1549, 1948.
13. Heaslet, Max A., Lomax, Harvard, and Jones, Arthur L.: Volterra's Solution of the Wave Equation as Applied to Three-Dimensional Supersonic Airfoil Problems. NACA TN No. 1412, 1947.

14. Hayes, W. D., Browne, S. H., and Lew, R. J.: Linearized Theory of Conical Supersonic Flow with Application to Triangular Wings. Rep. No. NA-46-818, Eng. Dept., North American Aviation, Inc., Sept. 30, 1946.
15. Lagerstrom, Paco A., Wall, D., and Graham, M. E.: Formulas in Three-Dimensional Wing Theory (1). Rep. No. SM-11901, Douglas Aircraft Co., Inc., July 1946.
16. Lagerstrom, P. A., and Graham, Martha E.: Downwash and Sidewash Induced by Three-Dimensional Lifting Wings in Supersonic Flow. Rep. No. SM-13007, Douglas Aircraft Co., Inc., April 1947.
17. Lagerstrom, P. A., and Graham, Martha E.: Linearized Theory of Supersonic Control Surfaces. Rep. No. SM-13060, Douglas Aircraft Co., Inc., July 24, 1947.
18. Evvard, John C.: Theoretical Distribution of Lift on Thin Wings at Supersonic Speeds (An Extension). NACA TN No. 1585, 1948.
19. Cohen, Clarence B., and Evvard, John C.: Graphical Method of Obtaining Theoretical Lift Distributions on Thin Wings at Supersonic Speeds. NACA TN No. 1676, 1948.
20. Brown, Clinton E., and Adams, Mac C.: Damping in Pitch and Roll of Triangular Wings at Supersonic Speeds. NACA TN No. 1566, 1948.
21. Moeckel, W. E., and Evvard, John C.: Load Distributions Due to Steady Roll and Pitch for Thin Wings at Supersonic Speeds. NACA TN No. 1689, 1948.
22. Heaslet, Max. A., and Lomax, Harvard: The Use of Source-Sink and Doublet Distributions Extended to the Solution of Arbitrary Boundary Value Problems in Supersonic Flow. NACA TN No. 1515, 1948.
23. Schlichting, H.: Airfoil Theory at Supersonic Speed. NACA TM No. 897, 1939.
24. Margolis, Kenneth: Supersonic Wave Drag of Sweptback Tapered Wings at Zero Lift. NACA TN No. 1448, 1947.
25. Ivey, H. Reese, and Bowen, Edward N., Jr.: Theoretical Supersonic Lift and Drag Characteristics of Symmetrical Wedge-Shaped-Airfoil Sections as Affected by Sweepback Outside the Mach Cone. NACA TN No. 1226, 1947.

26. Harmon, Sidney M., and Swanson, Margaret E.: Calculations of the Supersonic Wave Drag of Nonlifting Wings with Arbitrary Sweep-back and Aspect Ratio Wings Swept Behind the Mach Lines. NACA TN No. 1319, 1947.
27. Garrick, I. E., and Rubinow, S. I.: Theoretical Study of Air Forces on an Oscillating or Steady Thin Wing in a Supersonic Main Stream. NACA TN No. 1383, 1947.
28. Garrick, I. E., and Rubinow, S. I.: Flutter and Oscillating Air-Force Calculations for an Airfoil in a Two-Dimensional Supersonic Flow. NACA TN No. 1158, 1946.
29. Heaslet, Max. A., and Lomax, Harvard: Two-Dimensional Unsteady Lift Problems in Supersonic Flight. NACA TN No. 1621, 1948.
30. Peirce, B. O.: A Short Table of Integrals. Ginn and Co., 3d ed., 1929, p. 18.

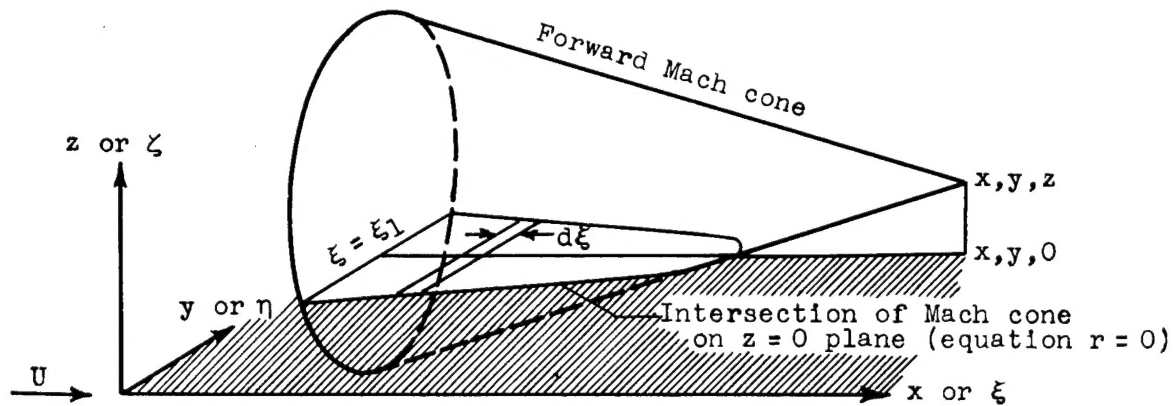


Figure 1. - Field of integration for evaluating velocity potential (equation (10)) of a source.

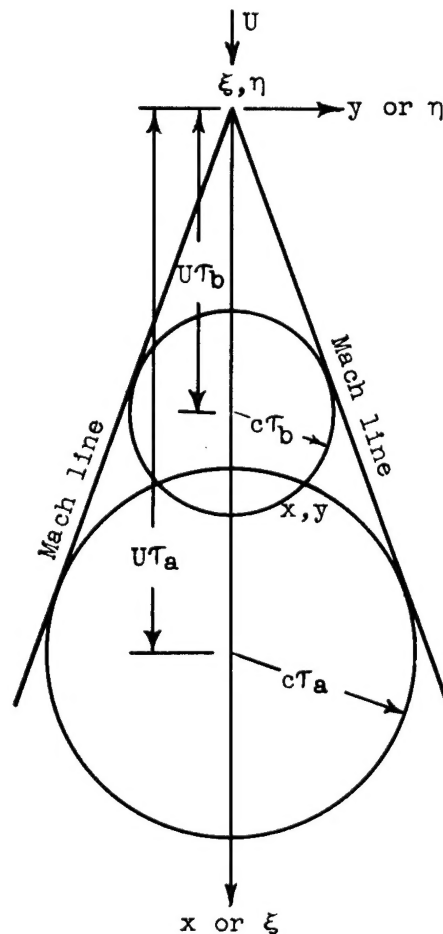


Figure 2. - Relation between time delays τ_a and τ_b and position of wave front.

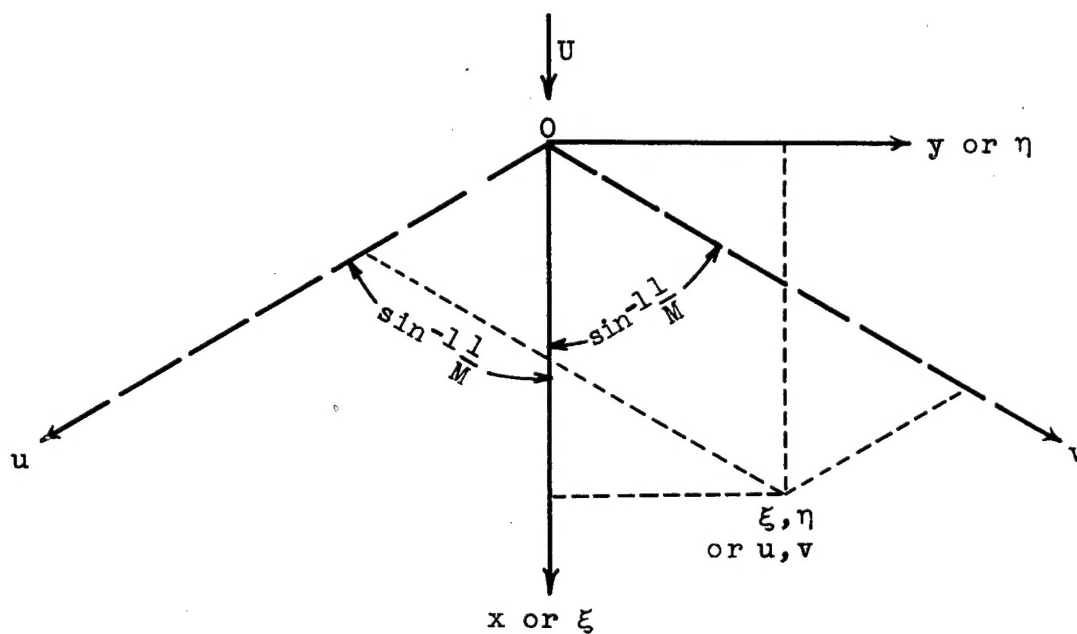


Figure 3. - Comparison of Cartesian and oblique coordinate systems.

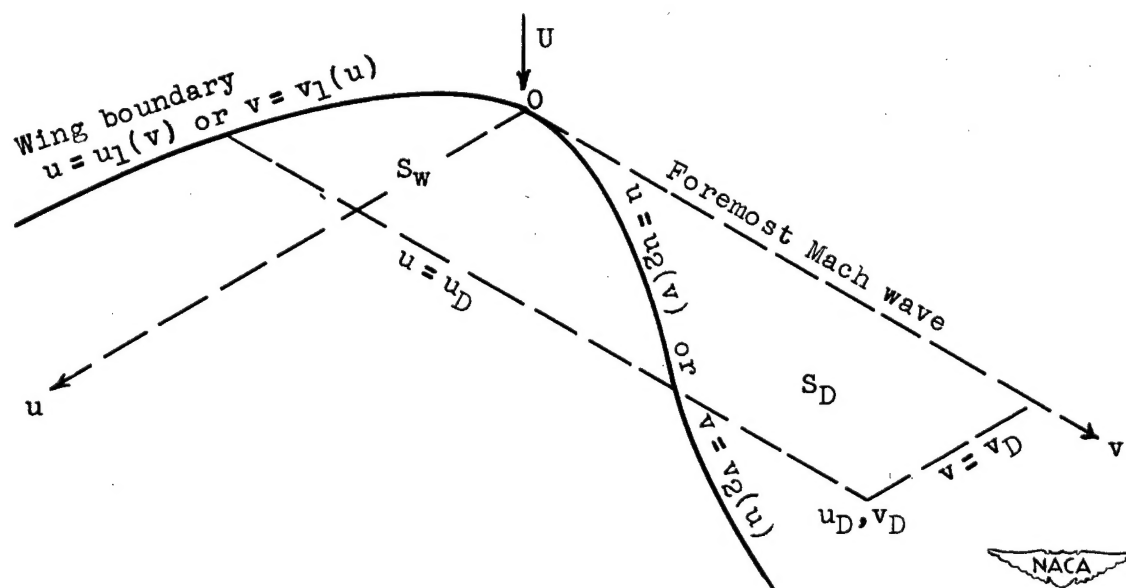


Figure 4. - Fields of integration for evaluating upwash between wing boundary and foremost Mach wave.

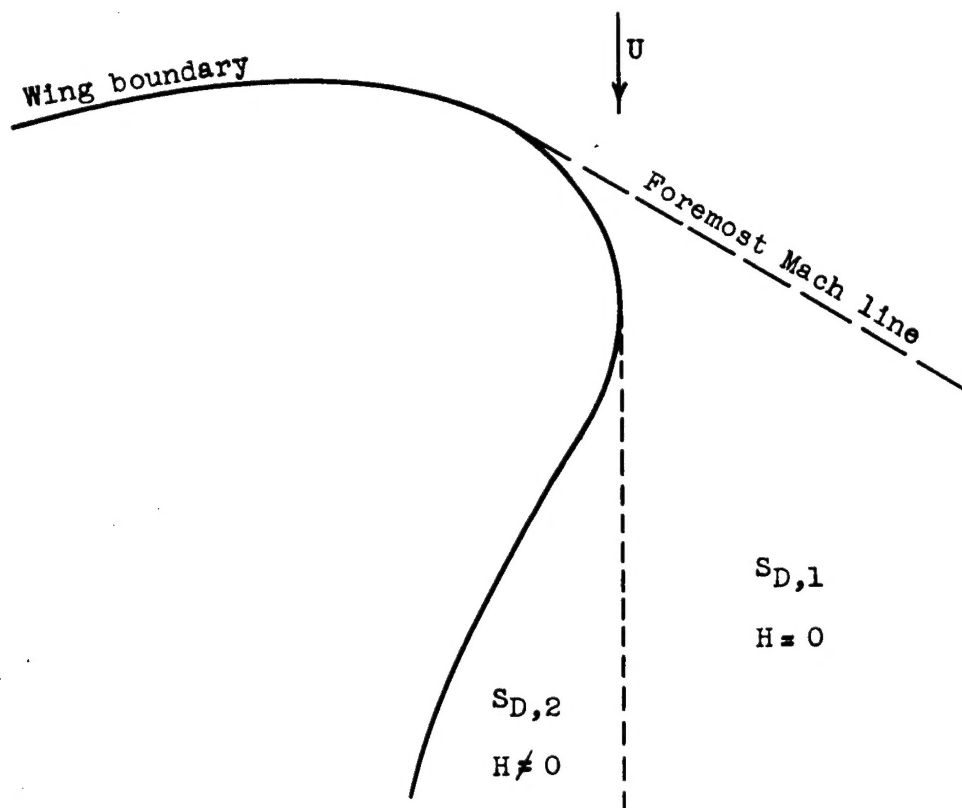


Figure 5. - Division of external field S_D for evaluation of H .

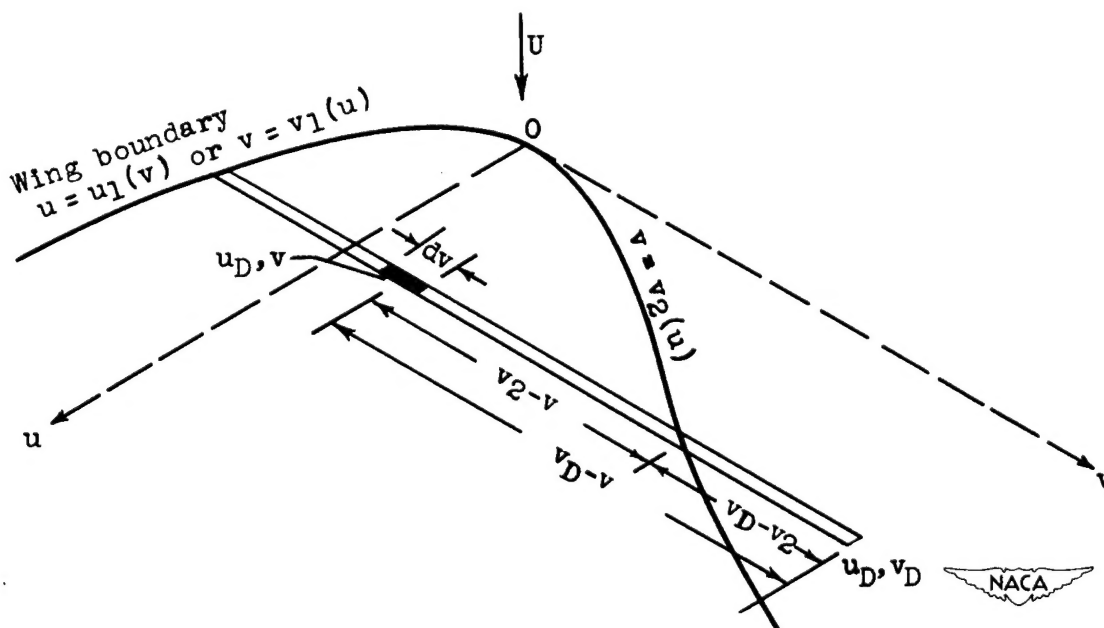


Figure 6. - Geometric significance of factors in equation (25).

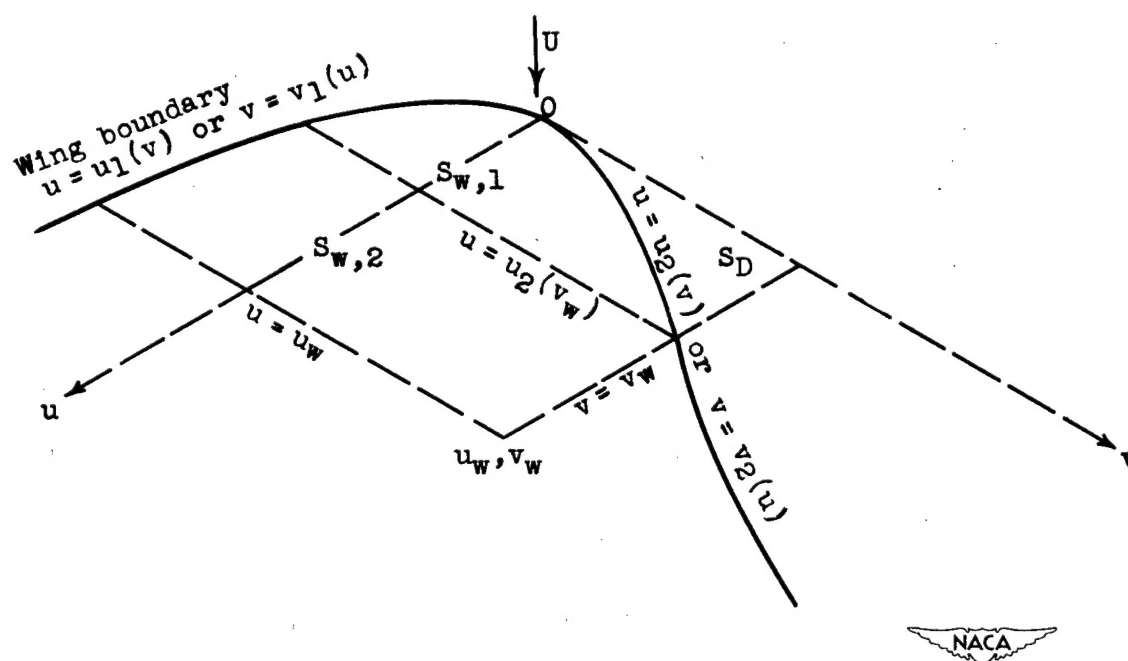


Figure 7. - Integration limits for equations (27) and (28).